Proceeding Paper
The GRB Afterglows Flowchart †

Esma Zouaoui * and Noureddine Mebarki

Laboratoire de Physique Mathématique et Subatomique, Frères Mentouri Constantine 1 University, BP, 325 Route de Ain El Bey, Constantine 25017, Algeria;
* Correspondence: esma.zouaoui@gmail.com
† Presented at the 2nd Electronic Conference on Universe, 16 February–2 March 2023; Available online: https://ecu2023.sciforum.net/.

Abstract: In this paper we present the flowchart of the Gamma-Ray Burst (GRB) afterglows, to create a numerical FORTRAN code. In the context of several proposed models, the hydrodynamic evolution describing the external shock of the jet with the environment surrounding of the GRB source or the Interstellar medium is discussed. A comparison of the results with data by considering the synchrotron emission as a basic mechanism for the radiation part was also made.

Keywords: GRB-afterglows; flowchart; hydrodynamic evolution; synchrotron emission

1. Introduction

" Gamma-Ray Bursts observations of a cosmic origin" is the title of the first article published in 1973 [1], when it was announced that it is the brightest event in the universe after the Bing Bang. Since that, many satellite missions and terrestrial projects were carried out to solve this enigma. One of these satellites called Beppo-SAX has confirmed definitively the cosmological origin of these bursts through the detection of the first remnant emission (afterglow) of the GRB970228 with a Redshift = 0.835 [2], defined as the external shock of the jet with the environment medium of the gamma rays burst's source [3]. Most of the theorists were focusing their studies on the fireball model [4,5], able to describe the external shock. In this purpose three hydrodynamic models in the literature were proposed describing the evolution of Lorentz factor; like the one of Chiang Dermer (1999) [6], Huang et al. (1999) [7] and Feng et al. (2002) [8], where the flowchart of these models will be presented later.

2. Hydrodynamic Evolution
2.1. Hydrodynamic Models

The bulk kinetic energy of the GRB fireball is expressed by [9]:

$$E_k = (\Gamma - 1)(M_0 + m)c^2 + \Gamma U \tag{1}$$

where Γ is bulk Lorentz factor of the deceleration, m the masse of the surrounding medium swept-up by the fireball. The radiated differential energy is given by [10]:

$$dE_{rad} = \varepsilon \Gamma (\Gamma - 1) dm c^2 \tag{2}$$

and

$$\varepsilon = \varepsilon_e \frac{t_{syn}^{'-1}}{t_{syn}^{'-1} + t_{ex}^{'-1}} \tag{3}$$

where ε is the fraction of internal energy radiated by the fireball [11,12], t_{syn}, t_{ex} are the synchrotron cooling and expansion times in the co-moving frame respectively and U is the Internal energy which is has many definitions proposed shown in the Table 1. Finally the

global conservation of energy is $dE_k = -dE_{rad}$, where the evolving of the Lorentz factor Γ to describe the hydrodynamic evolution of the GRBs Afterglows is resuming in the same Table 1.

Table 1. Different internal energy for each model its Lorentz factor evolution.

Models	Internal Energy		Lorentz Factor Evolution
Chaing [6]	$U = \int (\Gamma - 1)dm$	$dU = (\Gamma - 1)dm$	$\frac{d\Gamma}{dm} = -\frac{\Gamma^2 - 1}{M}$
Huang [7]	$U = (\Gamma - 1)mc^2$	$dU = (\Gamma - 1)dmc^2 + mc^2 d\Gamma$	$\frac{d\Gamma}{dm} = -\frac{\Gamma^2 - 1}{M_0 + \varepsilon m + 2(1-\varepsilon)\Gamma m}$
Feng [8]	$U = \int (1 - \varepsilon)dU_{ex}$	$dU = (1 - \varepsilon)dU_{ex} \backslash\backslash dU_{ex} = (\Gamma - 1)dmc^2 + mc^2 d\Gamma$	$\frac{d\Gamma}{dm} = -\frac{\Gamma^2 - 1}{M_0 + m + U/c^2 + (1-\varepsilon)\Gamma m}$

2.2. The Flowchart of the Hydrodynamic Evolution

The basic goal of this work is to draw a flowchart of the hydrodynamic evolution for the GRB afterglows then choose the most compatible model with the observational data (see Section 3.2), all steps for the first part are shown in Figure 1:
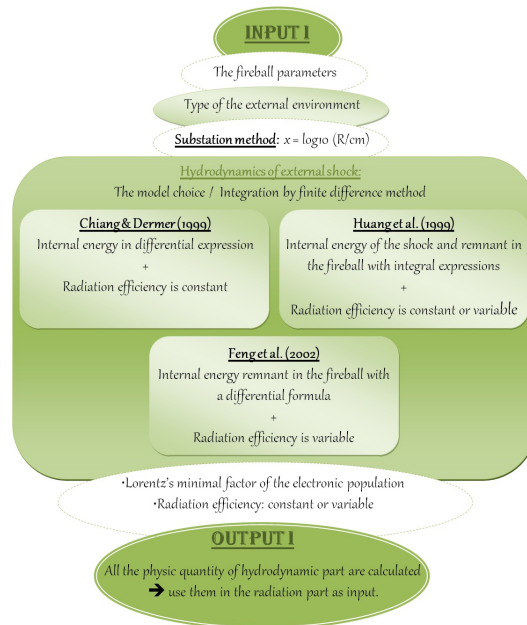

Figure 1. The flowchart of the hydrodynamic evolution of GRBs Afterglows.

- Starting with initial parameters for all necessary physical quantities: like those of the fireball and the external environment.
- Using the substitution $x = \log_{10} (R/cm)$ (logarithmic scale) suitable for large scales, dealing with large distances and time like the distance travel of a relativistic fireball jet and its radiation from the host galaxy to the earth.
- Specifying the state of the fireball whether it is radiated or not, constant or variable (depending on the effectiveness of the radiation). We will also choose a model of minimum Lorentz factor.
- Choosing the hydrodynamic model, then using the finite differences method as a numerical tool that approximate solutions of the Lorentz factor differential equations, as a function of the mass m of the surrounding medium sweeped-up by the fireball. In fact, this method appears to be the simplest one. Furthermore, using this method in our code gives results which converge to the Sedov solution [13], and also to the analytical solutions in the cases of an expanded and constant radiation.

3. Radiation Parte

3.1. Synchrotron Radiation and Self-Absorption

The synchrotron radiation power (OTS) at frequency ν' from all the accelerated electrons in the commoving frame is given by: [14]:

$$P_{\nu'} = \frac{2\sqrt{3}e^2\nu_L}{c}\int_{\Gamma_{min}}^{\Gamma_{max}} N_e'(\Gamma_e)F\left(\frac{\nu'}{\nu_c'}\right)d\Gamma_e \tag{4}$$

where $F(x)$ is the symchrotron function [15], ν_L is the Larmor frequency and N_e' is the electrons accelerated by the shock in the absence of radiation losses written as a bower low distribution [12]:

$$N_e'(\Gamma_e) = \frac{dN_e'}{d\Gamma_e} = C^{te}\Gamma_e^{-P}, \Gamma_{min} \leq \Gamma_e \leq \Gamma_{max} \tag{5}$$

where Γ_{max} (resp. Γ_{min}) is defined in [16,17] (resp. [18]).
Because of the cosmological nature of the GRBs we must use the relativistic transformations as [14,19]:

$$\nu = \frac{(1+\beta)\Gamma}{1+z}\nu' \tag{6}$$

$$d\Omega = \frac{1}{(1+\beta)^2\Gamma^2}d\Omega' \tag{7}$$

$$t_{obs} = (1+z)t \tag{8}$$

to get, the general expression for the instantaneous intensity in Jansky of synchrotron emission as a function of the luminosity distance $D_L(z)$ where z is the redshift:

$$(F_\nu)_{OTS} = \frac{1}{4\pi D_L(z)^2}4\pi\left(\frac{dP_\nu}{d\Gamma}\right)_{OTS} \tag{9}$$

The synchrotron self-absorption (SSA) at low frequencies plays an important role, where $\alpha_{\nu'}$ the optical depth is [20]:

$$\alpha_{\nu'} = \frac{(p+1)}{8\Pi m_e\nu'}\int_{\Gamma_{min}}^{\Gamma_{max}} P_e'(\Gamma_{\nu',e})\frac{N_e'(\Gamma_e)}{\Gamma_e}d\Gamma_e \tag{10}$$

so the instantaneous intensity for the SSA will be [21]:

$$\left(\frac{dP_\nu}{d\Gamma}\right)_{SSA} = \left(\frac{dP_\nu}{d\Gamma}\right)_{OTS}\frac{1}{\alpha_{\nu'}\Delta'}(1-e^{\alpha_{\nu'}\Delta'}) \tag{11}$$

3.2. The Flowchart of the Radiation Emission

In the second part (Figure 2), we produce the light curves represented by the intensity as a function of time Equation (9), Similarly for the afterglows spectra the samequantity as a function of the frequency.
Finally; the numerical curve presenting the frequency of the maximum mission in terms of $\nu F(\nu)$.

- To see the nature of the energy emitted by the afterglows as a function of time with the light curves, we introduce the frequency in the observations, then create a DO loop for various values of time to calculate the spectral intensity $F_\nu(t)$, In this loop we call the subroutines of the relativistic transformation for each distance R.
- For the spectra we do the opposite, that is we set the time then open a DO loop to evolve the frequency, and always call the subroutine of the relativistic transformation at every distance R.

- For the third calculations we make changes with two DO loops on the time and the frequency, and use the condition IF to save the frequency that gives the maximum of $\nu F(\nu)$.
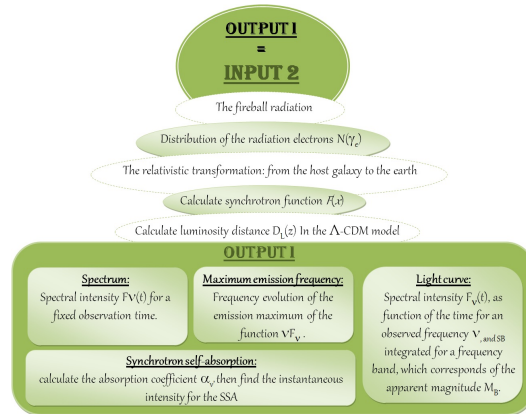

Figure 2. The flowchart of the Radiation of GRBs Afterglows.

To recognize this part, we use the $F(x)$ synchrotron function, to determine the spectral power, after the calculation of the distribution of the electrons radiating and respecting the numbers of the electrons which radiate or not(adiabatic electrons by which the characteristic time of the emission is very small compared to the time scales). We identify all the relativistic transformations representing the physical quantities in the host galaxy $(\nu', d\Omega)$ due to the cosmological distance as the luminosity distance $D_L(z)$. Finally, we calculate the absorption coefficient $\alpha_{\nu'}$ Equation (10) to get the instantaneous intensity for the SSA Equation (11) and present our results.

4. Numerical Results and Discussion

We have taken a fireball with an initial mass outflow, $M_0 = 2 \times 10^{-6} M_\odot$, Lorentz factor $\Gamma_0 = 65$ and a jet opening angle $\theta_{jet} = 10°$, a decelerating within the ISM with a constant density $n = 1$ cm^3 and $k = 0$ (n, k are parameters depending on the medium), $z = 3.645$, lateral expansion $g = 0$, numerical and spectral parameters $a = 4$ and $p = 2.3$ respectively. We have used also $\varepsilon_e = 0.1$, $\varepsilon_B = 0.9$ as the electronic and magnetic efficiencies with $\varepsilon_e + \varepsilon_B = 1$. The main goal of this code is to study and understand this phenomenon. In fact, from this flowchart we can highlight these most important results:

- Figure 3 shows that in the adiabatic expansion case the deceleration of the Lorentz factor is slower compared to that of a radiative regime generating a faster deceleration due to the radiation. Moreover, we can observe three sections of the deceleration corresponding to:
    1. The ultra-relativistic phase.
    2. The relativistic phase.
    3. The non-relativistic phase.
- Figure 4 displays the evolution of the radiative efficiency of the fireball e as a function of the distance R showing that the radiation in Haung's models more effective than in that of Feng.
- Figure 5 shows the ratio between the absorption coefficient $\alpha_{\nu'}$ for a radio frequency $\nu_{obs} = 3.10^8 Hz$ and an UV one $\lambda_{obs}^{-1} = 500 cm^{-1}$. Notice that it is more important in the low frequencies. This result is confirmed in Figure 6 where the spectra of GRB afterglow consist of a larger absorption in low frequencies than in higher ones.
- As a result from Figure 7 is that the majority of the radiations during of the GRB-afterglows emission are starting by the hard gamma to the radio bands. So the detection of the prompt emission of the GRBs is overlapped with the early afterglows

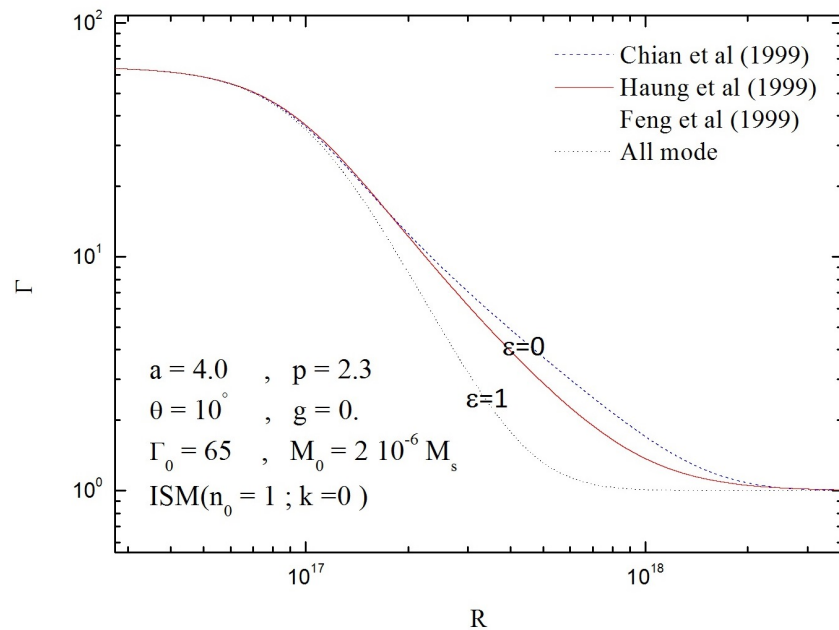- Figure 8 shows a good concordance with the data of the GRB170202 supporting the proposed model.

Figure 3. Evolution of the Lorentz factor Γ as a function of the distance R (in logarithmic scale). For radiative and adiabatic cases.
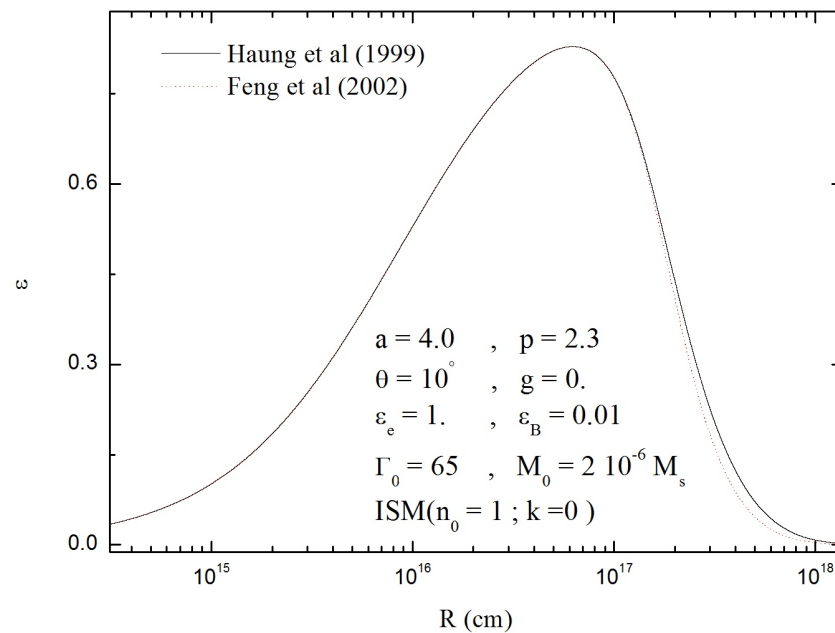

Figure 4. Evolution of the radiative efficiency of the fireball ε as a function of the distance R (in logarithmic scale).
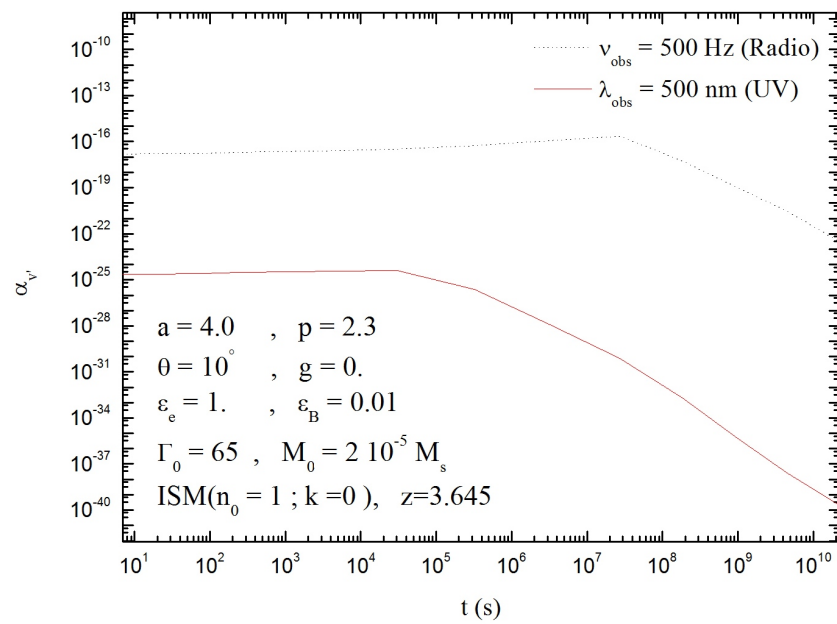
Figure 5. Evolution of absorption coeffcient $\alpha_{\nu'}$ for radio frequency and UV frequency (for Feng model).
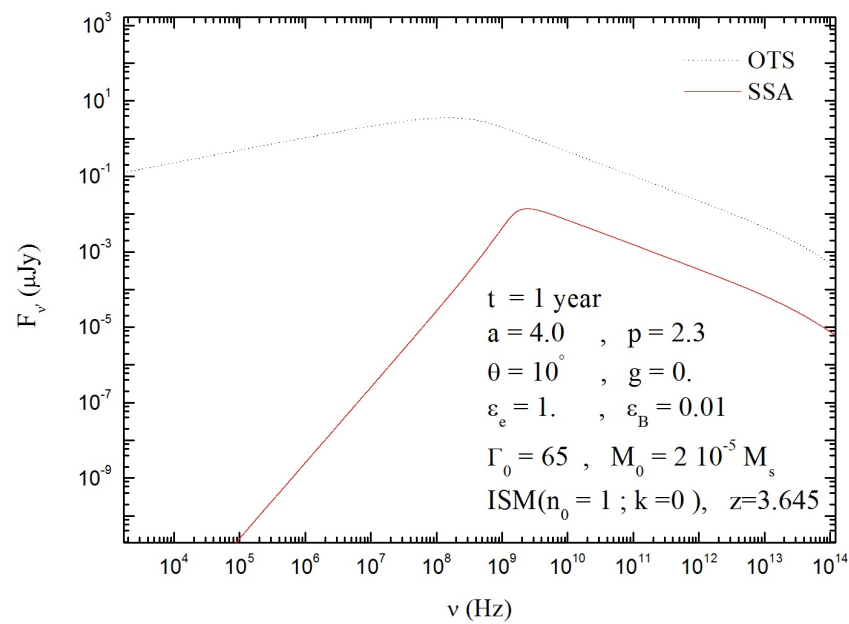
Figure 6. Spectra of GRB Afterglow in the two cases OTS and SSA emission (for Feng model).
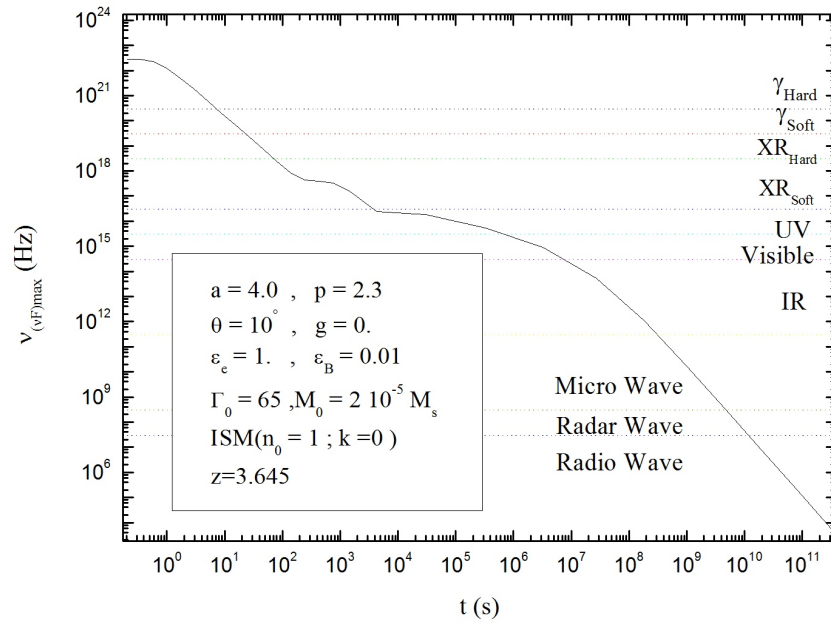
Figure 7. Frequency $\nu_{(\nu F)_{max}}$ corresponding to the maximum emission in terms of νF_{ν} as a function of the distance R (for Feng model).
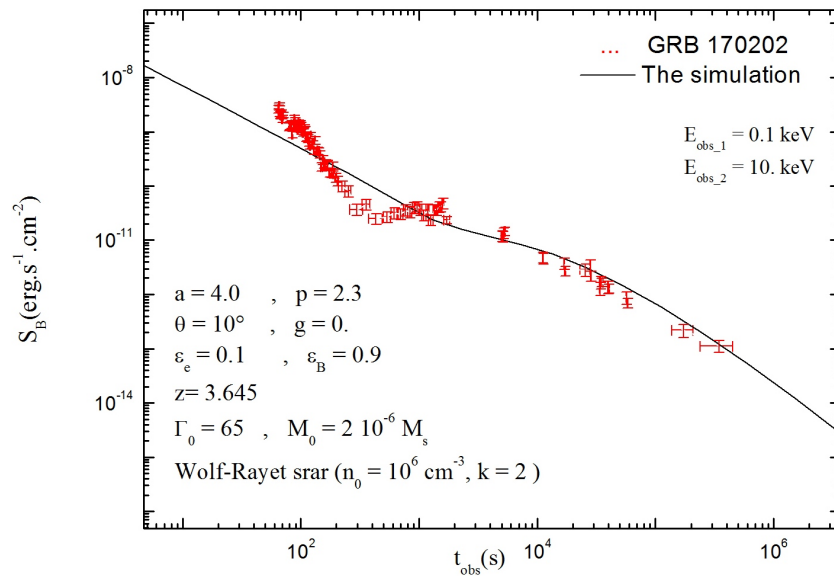

Figure 8. Comparison of calculated afterglow light curves (our code) to observed data by the XRT / Swift satellite in term of the integrated fluence, S_B (in erg.s^{-1}.cm^{-2} units) in the X-ray band ($E = 0.2$–10 keV).

5. Conclusions

In the presenter search work we have studied the evolving hydrodynamics of the afterglow and its emission where in the first part we have seen that the Feng's model is the most interesting one [22,23]. From the point of view of the efficiency, the latter changes during the evolution of the fireball, which makes it more realistic to describe the internal energy. It is worth to mention that the Feng models consistent with the Sedov solution both the non-relativistic phase and adiabatic regime. In the second part we have studied the basic radiation of the GRB afterglow by the synchrotron emission which is not negligible. The self synchrotron absorption as an effect which plays important role in the low frequency

range giving a fairly good approximation to the real data as in our case where the profile of the GRB 170202 afterglow was detected by Swift/XRT.

References

1. Klebesadel, R.W.; Strong, I.B.; Olson, R.A. Olson, Observation of Gamma-Ray Bursts of Cosmic Origin. *Astrophys. J.* **1973**, *182*, L85–L88.
2. Costa, E.; Frontera, F.; Heise, J.; Feroci, M.; in 't Zand, J.; Fiore, F.; Cinti, M.N.; Fiume, D.D.; Nicastro, L.; Orlandini, M.; et al. Discovery of an X-ray afterglow associated with the γ-ray burst of 28 February 1997. *Nature* **1997**, *387*, 783–785.
3. Shaviv, N.J.; Dar, A. Fireballs in dense stellar regions as an explanation of gamma-ray bursts. *Mon. Not. R. Astron. Soc.* **1995**, *277*, 287–296.
4. Sari, R.; Piran, T. Variability in gamma-ray bursts: A clue. *Astrophys. J.* **1997**, *485*, 270–273.
5. Dermer, C.D.; Mitman, K.E. Short-timescale variability in the external shock model of gamma-ray bursts. *Astrophys. J.* **1999**, *513*, L5–L8.
6. Chiang, J.; Dermer, C.D. Synchrotron and synchrotron self-compton emission and the blast-wave model of gamma-ray bursts. *Astrophys. J.* **1999**, *512*, 699–710.
7. Huang, Y.F.; Dai, Z.G.; Lu, T. A generic dynamical model of gamma-ray burst remnants. *Mon. Not. R. Astron. Soc.* **1999**, *309*, 513–316.
8. Feng J.B.; Huang, Y.F.; Dai, Z.G.; Lu, T. Dynamical evolution of gamma-ray burst remnants with evolving radiative efficiency. *Chin. J. Astron. Astrophys.* **2002**, *2*, 525–532.
9. Panaitescu, A.; Mészáros, P.; Rees, M.J. Multiwavelength afterglows in gamma-ray bursts: Refreshed shock and jet effects. *Astrophys. J.* **1998**, *503*, 314–315.
10. Blandford, R.D.; McKee, C.F. Fluid dynamics of relativistic blast waves. *Phys. Fluids* **1976**, *19*, 1130–1138.
11. Dai, Z.G.; Lu, T. Gamma-ray burst afterglows: effects of radiative corrections and non-uniformity of the surrounding medium. *Not. R. Astron. Soc.* **1998**, *298*, 87–92.
12. Dai, Z.G.; Huang, Y.F.; Lu, T. Gamma-ray burst afterglows from realistic fireballs. *Astrophys. J.* **1999**, *520*, 634–640.
13. Sedov, L. *Similarity and Dimensional Methods in Mechanics*; Ch. IV; Academic: New York, NY, USA, 1969.
14. Rybicki, G.B.; Lightman, A.P. *Radiative Processes in Astrophysics*; Wiley and Sons: New York, NY, USA, 1979.
15. Abramowiotz, M.; Stegum, I.A. *Handbook of Mathematical Function*; Dover: New York, NY, USA, 1965.
16. De jager, O.C.; Harding, A.K. The expected high-energy to ultra-high-energy gamma-ray spectrum of the Crab Nebula. *Astrophys. J.* **1992**, *4396*, 161–172.
17. De Jager, O.C.; Harding, A.K.; Michelson, P.F.; Nel, H.I.; Nolan, P.L.; Sreekumar, P. Gamma-Ray Observations of the Crab Nebula: A Study of the Synchro-Compton Spectrum. *Astrophys. J.* **1996**, *457*, 253–266.
18. Sari, R.; Piran, T.; Narayan, R. Spectra and light curves of gamma-ray burst afterglows. *Astrophys. J. Lett.* **1998**, *497*, L17–L20.
19. Lind, K.R.; Blandford, R.D. Semidynamical models of radio jets-Relativistic beaming and source counts. *Astrophys. J.* **1985**, *295*, 358–367.
20. Jonathan, G.; Tsvi, P. Reém, S. Synchrotron self-absorption in gamma-ray burst afterglow. *Astrophys. J.* **1999**, *527*, 236–246.
21. Zouaoui, E.; Mebarki, N. Synchrotron Emission and Self-Absorption in GRB Afterglows. *J. Phys. Conf. Ser.* **2019**, *1269*, 012010.
22. Zouaoui, E.; Fouka, M.; Ouichaoui, S. Hydrodynamical Evolution of GRBs Afterglows: Realistic model with evolving radiative efficiency. *Aip Conf. Proc.* **2012**, *1444*, 359–362.
23. Zouaoui, E.; Fouka, M.; Ouichaoui, S. Sciences & Technologie. A sciences exactes. **2015**, *41*, 71–74.